Fixed switching frequency and three level inverter to improve the performance of sensorless PMSM

DOI : 10.36909/jer.14285

*Hamdy Mohamed Soliman

*Department of Electrical Power and Machine Engineering, Faculty of Engineering, Misr University for science and Technology, 6th October, Giza, Egypt.

*Email: eldoctorhamdy70@gmail.com; Corresponding Author.

ABSTRACT

The vector control drive system is a very important method to get high dynamic performance. To increase the reliability and decrease the cost of this system, the sensorless speed control is used. Here sensorless speed control conventional model reference adaptive system was studied. It was studied due to have many advantages. Although it has many advantages, but also, it has some drawbacks. These drawbacks an increase in the torque ripples, an increase in distortion of the stator currents, fluxes and motor speed. The aim of this paper is beating the drawbacks of the chosen system through simulation only. Three level inverter with space vector modulation constant switching frequency is used to overcome these drawbacks. To show the effect of the proposed system, it was compared to the conventional system. The conventional system here uses the two-level inverter with space vector modulation. To show the advantages of the constant switching frequency, the three-level inverter was used without keeping the constant switching frequency. The comparison held among the conventional model, the improved model which using the three-level inverter only and proposal model (the three-level inverter which using constant switching frequency). In the conventional model, the reference currents and the estimating currents compared to generate the reference voltage of the space vector modulation. In proposal model, the stator fluxes were estimated and compared to the reference stator fluxes to generate the same voltage of the space vector modulation through keeping the switching time constant. The simulation results proved that importance of the proposed model to improve the drawbacks of the conventional model reference adaptive system.

Key words: model reference adaptive system; sensorless drive system; space vector modulation; Three level inverter.

INTRODUCTION

The permanent magnet synchronous motor (PMSM) has many advantages so, it is spread in the many industrial applications. There are many methods to get high dynamic performance from PMSM. From the best control methods to get high dynamic performance, the vector control (Tingting et al., 2014; Kangping et al., 2014) so, this method is chosen here. To get

good switching sequence to drive the PMSM, the position sensor is required. Using the position sensor will increase the cost, increase the maintenance and reduce the reliability. To beat the sensor problems, the control system can be converted from sensor to sensorless (Shweta et al., 2018; Omer et al., 2018). In sensorless control, the voltage sensor and current sensor used to estimate the speed and position of the PMSM. The sensorless methods can be classified into open loop and closed loop sensorless controls.

1- The motor speed and its position in open loop sensorless can be estimated by many methods (Sandeepet al., 2018). These methods can be summarized in the follows;

The first method called the direct calculations method. It depends upon the measured values of the voltages and currents, but this method is directly related to the machine parameters and more effecting by noise resulting from the measurements.

In the second method, the position and motor speed can be calculated depending upon the variation of motor inductance and saturation effect. This technique used to calculate the motor position at the standstill.

Another method used the back EMF to estimate the motor speed and motor position. This method of control is suitable to calculate motor speed and motor position at medium and high speed.

The methods of the speed control of the PMSM with sensorless in case of open loop aren't suitable for high performance applications because the motor parameters are varying with continuity of operation and these variations don't take into consideration.

2- Other methods of the sensorless of the speed control (the closed loop to speed control of the PMSM without sensor) are more accurate if it is compared to the open loop control methods due to effect of feedback. These methods can be summarized as the following.

(Shoeb Hussain and Mohammad Abid Bazaz, 2016; Abolfazl et al., 2015) use the artificial neural networks to estimate the motor speed and its position, but this method needs more experience and needs a fast processor.

(Yuxin et al., 2020) used high signal injection methods to operate the PMSM. These methods are very good methods when the motor operated under low frequency, but these methods aren't suitable with medium speed and with higher speed.

(Shoeb Hussain and Mohammad Abid Bazaz, 2014) used extend Kalman filter to estimate the motor position and its speed, but these methods need more time in the calculations and it is a more complex method if it is compared to the other methods.

(Sandeep et al., 2020) used the back EMF to estimate the rotor position, but this method when used with low speed, the value of back EMF is a very small and its maybe can't measure correctly.

(Qing et al., 2013; Hongguo et al., 2018) use the sliding mode control to estimate the motor speed. This method is a very good method, but it may be suffering from the scattering phenomena.

(Abbas et al., 2020; Zhewen et al., 2020) use the fuzzy logic controller to estimate the motor speed, but this method needs more training and more experience.

(AMOR et al., 2020) used some models reference adaptive system to estimate the motor position and its speed, but the classical methods in this branch generate noise, harmonics, and ripple in the motor performance.

In this paper, the model reference adaptive system (MRAS) was used to drive the PMSM through vector control because it is an easy implementation. To overcome the problems for this model, the three-level space vector modulation with constant frequency was used. To appear the importance of this model, the classical model was used, the classical model with space vector modulation three level inverter was used and the proposed model was used. When comparing between these models through simulation, it was found that with the proposed model, the performance characteristics of the PMSM become the best if it is compared to the

other models. where it is found that the motor torque ripples decrease, the distortion in the flux decrease, the total harmonics distortion decrease and the noise in the speed vanish.
This paper is organized as; introduction, mathematical model of PMSM, classical sensorless model, first modified model, proposal model, simulation results and conclusions.

Mathematical model of the PMSM

The mathematical model of the three phase PMSM can be written as;

$$\frac{d}{dt}\begin{bmatrix} I_q \\ I_d \\ \omega_r \end{bmatrix} = \begin{bmatrix} \frac{-R_S}{L_q} & \frac{-L_d}{L_q} P\omega_r & \frac{-P\lambda_m}{L_q} \\ \frac{L_q}{L_d} P\omega_r & \frac{-R_S}{L_d} & 0 \\ \frac{3P}{2J}\lambda_m & \frac{I_q}{J}(L_d - L_q) & \frac{-B}{J} \end{bmatrix} \begin{bmatrix} I_q \\ I_d \\ \omega_r \end{bmatrix} + \begin{bmatrix} \frac{1}{L_q} & 0 & 0 \\ 0 & \frac{1}{L_d} & 0 \\ 0 & 0 & \frac{-1}{J} \end{bmatrix} \begin{bmatrix} V_q \\ V_d \\ T_L \end{bmatrix} \quad (1)$$

Where I_d and I_q are the dq-axes currents. V_d and V_q are the dq-axes voltages, L_d and L_q are the dq-axes inductances, R_S is the stator resistance per phase, λ_m is the rotor permanent magnet flux, P is the number poles pair, J is the moment of inertia, B is fractional coefficient, T_L is the load torque and ω_r is rotor speed.

Classical sensorless model

Figure 1 shows the classical sensorless block diagram of the PMSM through vector control. In this model, * means the reference value and ^ means the estimating value. Also, this model can be explained as, the reference speed was compared to the estimating speed and the error between them is the input to the PI speed controller. The output of the PI speed controller is the reference q-axis stator current. This reference was compared to the q-axis stator current which estimating from MRAS and the error between them is the input to the PI current controller. Also, the d-axis reference stator current deduces from lookup table with the help of the motor speed which estimating from the MRAS. This reference current is compared to d-axis stator current which estimating from the MRAS and the error between them was applied to the input of the other PI current controller. The outputs of the two PI's current controller are converted into two phase voltages in the stationary reference frame with help of estimating position sensor. These two-phase voltages in the stationary reference frame used to create two level pulses to drive the inverter through space vector pulse width modulation (SVPWM). The output voltages of inverters are applied to the PMSM to drive it. The SVPWM used to generate the pulses to drive the inverter. The number of states with this method are eight states. Two of them is the zero voltage vectors (V_0,V_7) and the others are non-zero voltage vectors (V_1-V_6) (Hamdy M. Soliman, 2019). All voltage vectors can be deduced from the following

$$V_n = \begin{cases} \frac{2}{3} V_{DC} e^{j(n-1)\frac{\Pi}{3}} & \text{for } n = 1,2,3,4,5,6 \\ 0 & \text{for } n = 0 \text{ and } 7 \end{cases} \quad (2)$$

The diagram of the general voltage vector can be seen in figure 2. From this figure can be concluded that the average output voltage of the inverter (v_{ref}) can be estimated depending upon any two adjacent voltage vectors (v_n, v_{n+1}) with any zero-voltage vector (V_0 orV_7) and time duration for each voltage vector (T_{vn}, T_{vn+1}) and total switching time (T_s). This can be expressed as;

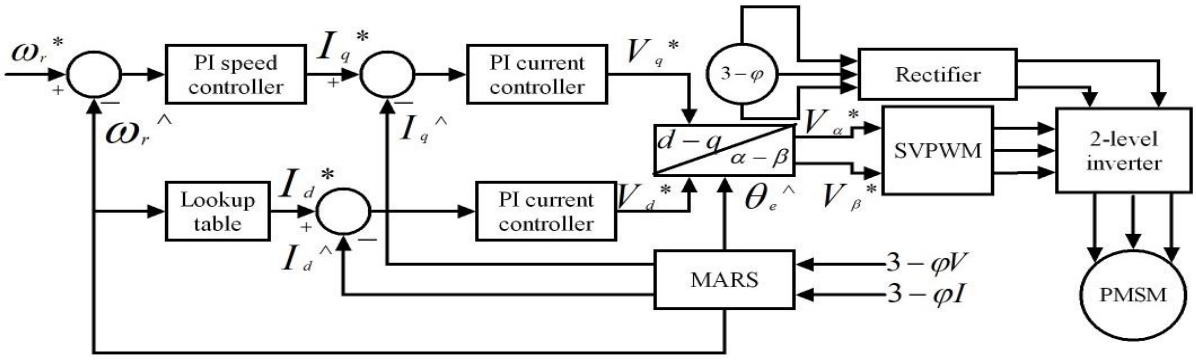

Figure 1 Classical sensorless block diagram of the PMSM through vector control

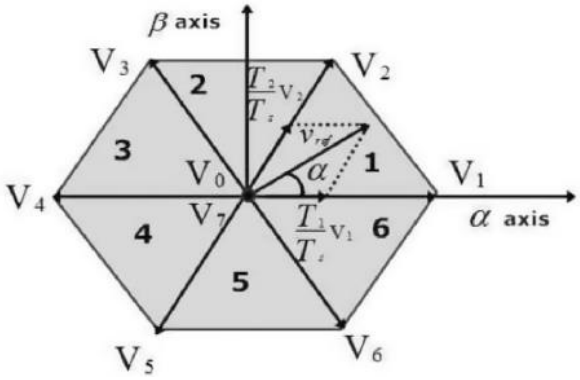

Figure 2 The general diagram of the voltages vector

$$v_{ref} = \frac{T_{vn} v_n + T_{vn+1} v_{n+1}}{T_s} \tag{3}$$

The time duration of the voltage vectors at any instant can be calculated as,

$$T_{vn} = \frac{\sqrt{3}|v_{ref}|T_s}{v_{DC}}\left[\sin(\frac{n\Pi}{3} - \theta)\right]$$
$$T_{vn+1} = \frac{\sqrt{3}|v_{ref}|T_s}{v_{DC}}\left[\sin(\frac{(n-1)\Pi}{3} - \theta)\right] \tag{4}$$
$$T_{v0,v7} = T_s - T_{vn} - T_{vn+1}$$

Depending upon eq. (4), the switching time for each switch of inverter from s_1 to s_6 can be written as in the table I. Also, the output voltages of the inverter line to line and phase voltage can be written as;

Table I Switching time of inverter for each switch

Sector	Upper switches	Lower switches
1	$s_1 = T_1 + T_2 + \frac{T_0}{2}, s_3 = T_2 + \frac{T_0}{2}, s_5 = \frac{T_0}{2}$	$s_2 = \frac{T_0}{2}, s_4 = T_2 + \frac{T_0}{2}, s_6 = T_1 + T_2 + \frac{T_0}{2}$
2	$s_1 = T_2 + \frac{T_0}{2}, s_3 = T_1 + T_2 + \frac{T_0}{2}, s_5 = \frac{T_0}{2}$	$s_2 = T_2 + \frac{T_0}{2}, s_4 = \frac{T_0}{2}, s_6 = T_1 + T_2 + \frac{T_0}{2}$
3	$s_1 = T_1 + T_2 + \frac{T_0}{2}, s_3 = T_2 + \frac{T_0}{2}, s_5 = \frac{T_0}{2}$	$s_2 = T_1 + T_2 + \frac{T_0}{2}, s_4 = T_2 + \frac{T_0}{2}, s_6 = \frac{T_0}{2}$
4	$s_1 = \frac{T_0}{2}, s_3 = T_2 + \frac{T_0}{2}, s_5 = T_1 + T_2 + \frac{T_0}{2}$	$s_2 = T_1 + T_2 + \frac{T_0}{2}, s_4 = T_2 + \frac{T_0}{2}, s_6 = \frac{T_0}{2}$
5	$s_1 = T_2 + \frac{T_0}{2}, s_3 = \frac{T_0}{2}, s_5 = T_1 + T_2 + \frac{T_0}{2}$	$s_2 = T_2 + \frac{T_0}{2}, s_4 = T_1 + T_2 + \frac{T_0}{2}, s_6 = \frac{T_0}{2}$
6	$s_1 = T_1 + T_2 + \frac{T_0}{2}, s_3 = \frac{T_0}{2}, s_5 = T_2 + \frac{T_0}{2}$	$s_2 = \frac{T_0}{2}, s_4 = T_1 + T_2 + \frac{T_0}{2}, s_6 = T_2 + \frac{T_0}{2}$

The line-to-line voltages and phase voltages (v_{ab}, v_{bc}, v_{ca} and v_{an}, v_{bn}, v_{cn}) can be written as the follows;

$$\begin{bmatrix} v_{ab} \\ v_{bc} \\ v_{ca} \end{bmatrix} = v_{DC} \begin{bmatrix} 1 & -1 & 0 \\ 0 & 1 & -1 \\ -1 & 0 & 1 \end{bmatrix} \begin{bmatrix} a \\ b \\ c \end{bmatrix} \quad (5)$$

$$\begin{bmatrix} v_{an} \\ v_{bn} \\ v_{cn} \end{bmatrix} = \frac{v_{DC}}{3} \begin{bmatrix} 2 & -1 & -1 \\ -1 & 2 & -1 \\ -1 & -1 & 2 \end{bmatrix} \begin{bmatrix} a \\ b \\ c \end{bmatrix} \quad (6)$$

Depending upon eqs. (5-6), the switching state, phase voltages and line to line voltages can be written as in table II.

Table II Switching state and corresponding phase and line to line voltages

Voltage vector	Switching on	Line to neutral voltages			Line to line voltage		
		v_{an}	v_{bn}	v_{cn}	v_{ab}	v_{bc}	v_{ca}
V_0	T_1, T_3, T_5	0	0	0	0	0	0
V_1	T_2, T_3, T_5	2/3	−1/3	−1/3	1	0	−1
V_2	T_2, T_4, T_5	1/3	1/3	−2/3	0	1	−1
V_3	T_1, T_4, T_5	−1/3	2/3	−1/3	−1	1	0
V_4	T_1, T_4, T_6	−2/3	1/3	1/3	−1	0	1
V_5	T_1, T_3, T_6	−1/3	−1/3	2/3	0	−1	1
V_6	T_2, T_3, T_6	1/3	−2/3	1/3	1	−1	0
V_7	T_2, T_4, T_6	0	0	0	0	0	0

Also, the estimating stator currents in the rotating reference frame, motor speed and motor position depend upon the classic model reference adaptive system (MRAS). This model can be explained as the following;

The general view of the MRAS block diagram can be seen in figure 3. From this figure can be concluded that the MRAS consists of the reference model, adjustable model and PI controller for performing adaptation. The reference model is used to calculate dq-axes stator currents (I_d, I_q) and voltages (V_d, V_q) in the rotating reference frame. It depends upon the measuring three phase voltages ($3\varphi V$), currents ($3\varphi I$) and the estimating rotor position ($\theta_e^{\wedge}$) of the motor. The details of the adjustable model can be seen in figure 4. This block can be represented by the following algorithm.

$$\frac{d}{dt}\begin{bmatrix} I_q^{AM} \\ I_d^{AM} \end{bmatrix} = \begin{bmatrix} \frac{-R_S}{L_q} & \frac{-L_d}{L_q}\omega_e^{\wedge} & \frac{-P\lambda_m}{L_q} \\ \frac{L_q}{L_d}\omega_e^{\wedge} & \frac{-R_S}{L_d} & 0 \end{bmatrix} \begin{bmatrix} I_q^{AM} \\ I_d^{AM} \\ \omega_e^{\wedge} \end{bmatrix} + \begin{bmatrix} \frac{1}{L_q} & 0 \\ 0 & \frac{1}{L_d} \end{bmatrix} \begin{bmatrix} V_q \\ V_d \end{bmatrix} \quad (7)$$

Where I_d^{AM}, I_q^{AM} are the d-q axes stator currents resulting from adjustable model and $\omega_e^{\wedge}$ is the estimating frequency resulting from modeling reference adaptive system.

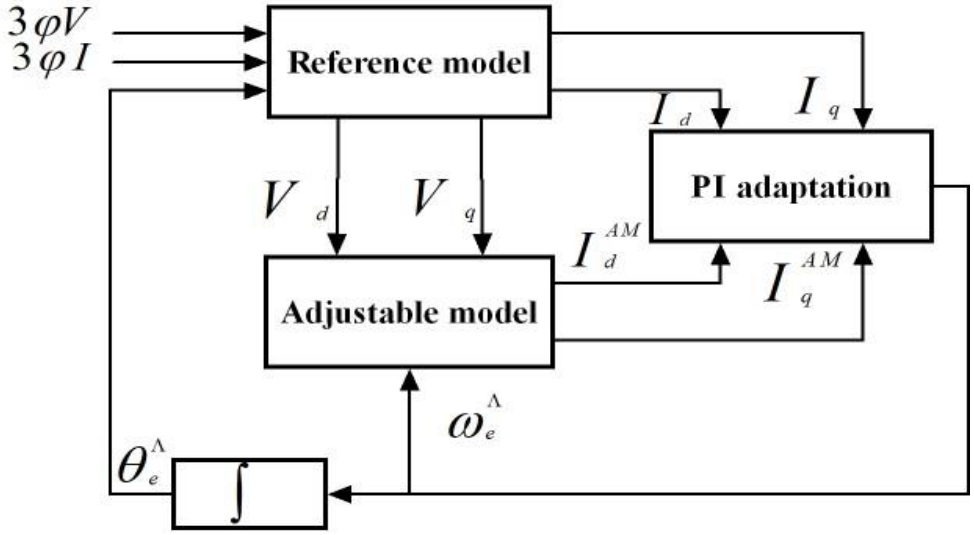

Figure 3 Block diagram of MRAS

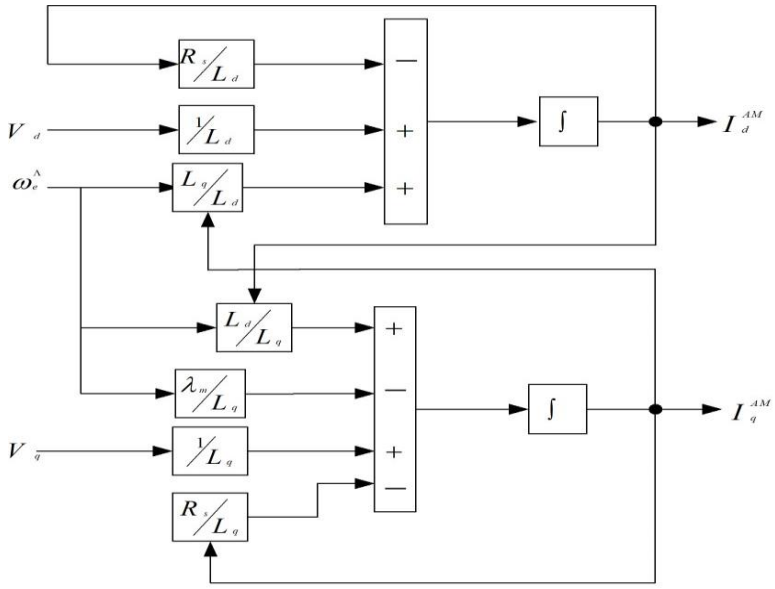

Figure 4 Adjustable model of MRAS

The details of PI adaptation model to calculate the motor speed and its position can be seen in figure 5. This can be expressed by the following;

$$\omega_e^{\Lambda} = \Delta e k_p + \int \Delta e k_i \, dt$$
$$\Delta e = I_d I_q^{AM} - I_q I_d^{AM} + \frac{\lambda_m}{L_d}(I_q^{AM} - I_q) \quad (8)$$

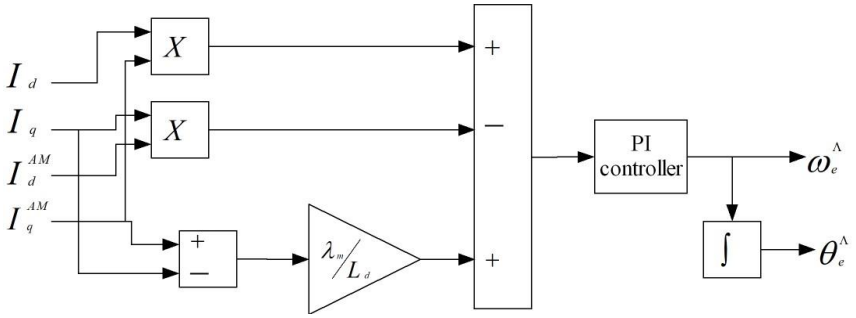

Figure 5 PI adaptation model

Modified sensorless model

Here the modified sensorlss means replace the two-level inverter by three level inverter. The inverter type used here is the neutral point clamped inverter. It was used due to has many advantages if it is compared to the two-level inverter as; low electromagnetic interface, low total harmonic distortion, high level output voltage and high efficiency (Zulkifilie et al., 2014). This inverter can be seen in figure 6. In this configuration, when the switches s_{1a} and s_{2a} turned on, the output voltage becomes $\frac{V_{DC}}{2}$, when the switches s_{3a} and s_{4a} turned on, the output voltage becomes $-\frac{V_{DC}}{2}$ and when the switches s_{3a} and s_{2a} turned on, the output voltage becomes zero. The number of states for these switches are 27. The shape of the SVPWM for this inverter can be seen in figure7.

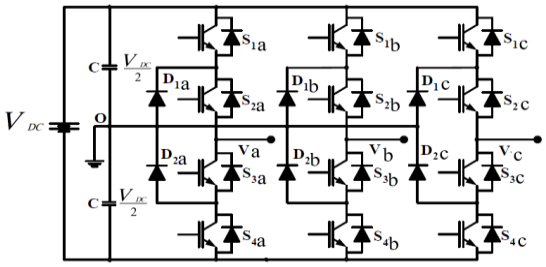

Figure 6 Three level inverter

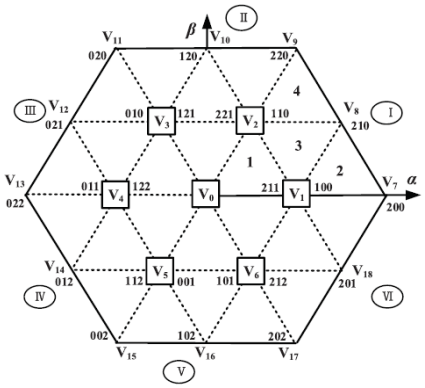

Figure 7 SVM for the three-level inverter

The vector voltage can be seen as; center vectors (three vectors), middle vectors (twelve vectors), internal vectors (six vectors) and external vector voltages (six vectors). Also, from this figure, it is found that the plain of the SVM is divided into six sector each sector contains four triangles. The on-time calculation can be estimated for each triangle in the plane. Here the on-time calculation for sector one can be calculated as an example depending upon figure 8 as;

$$V_{ref} = \frac{V_8 T_a + V_1 T_b + V_7 T_c}{T_S} \qquad (9)$$

$$T_S = T_a + T_b + T_c$$

Depending upon figure 8 and eq. (9) the on-time can be calculated as in table II where

$$a = \frac{3T_s V_{ref}}{V_{DC}}$$

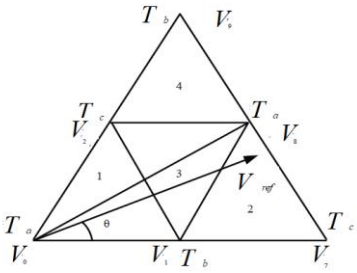

Figure 8 Vector voltage and on-time turn

Also, the corresponding phase voltage can be written as;

$$\begin{bmatrix} V_{an} \\ V_{bn} \\ V_{cn} \end{bmatrix} = \begin{bmatrix} 2 & -1 & -1 \\ -1 & 2 & -1 \\ -1 & -1 & 2 \end{bmatrix} \begin{bmatrix} S_{1a} \\ S_{1b} \\ S_{1c} \end{bmatrix} + \begin{bmatrix} 2 & -1 & -1 \\ -1 & 2 & -1 \\ -1 & -1 & 2 \end{bmatrix} \begin{bmatrix} S_{2a} \\ S_{2b} \\ S_{2c} \end{bmatrix} \quad (10)$$

The line to line voltages can be written as;

$$V_{ab} = V_{an} - V_{bn},\ V_{bc} = V_{bn} - V_{cn},\ V_{ca} = V_{cn} - V_{an} \quad (11)$$

Table III On-time calculation for sector one

	t_a	t_b	t_c
Region 1	$T_s - a\sin(\theta + \pi/3)/\sqrt{3}$	$-a\sin(\theta - \pi/3)/\sqrt{3}$	$a\sin\theta/\sqrt{3}$
Region 2	$a\sin\theta/\sqrt{3}$	$2T_s - a\sin(\theta + \pi/3)/\sqrt{3}$	$-T_s - a\sin(\theta - \pi/3)/\sqrt{3}$
Region 3	$-T_s + a\sin(\theta + \pi/3)/\sqrt{3}$	$T_s - a\sin\theta/\sqrt{3}$	$T_s + a\sin(\theta - \pi/3)/\sqrt{3}$
Region 4	$-a\sin(\theta - \pi/3)/\sqrt{3}$	$-T_s + a\sin\theta/\sqrt{3}$	$2T_s - a\sin(\theta + \pi/3)/\sqrt{3}$

Proposal sensorless model

The block diagram of the proposed method of the PMSM through vector control can be seen in figure 9. The type of inverter used here is the same inverter in the modified model but the switching frequency was kept constant. Keeping switching frequency constant will more improve the output of the classical sensorless model which reflect the motor performance overall if it is compared to both models (classical model and modified model). This method of control can be explained as follows;

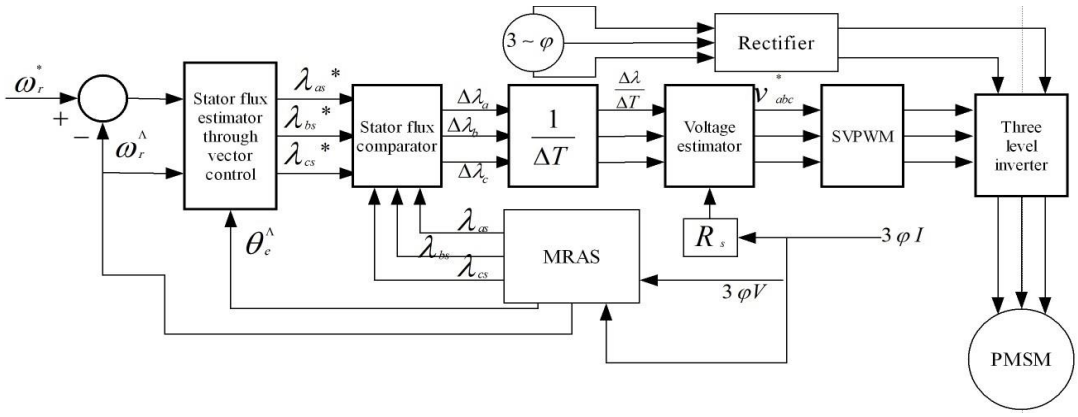

Figure 9 Proposal sensorless block diagram of the PMSM through vector control

The reference motor speed was compared to the estimated speed (come from classical MRAS) and the error between them is the input to stator flux estimator through vector block. Details of this block can be seen in figure 10. The output of this block is referenced stator flux in the stationary reference frame. This flux was compared to the estimating stator flux computed from MRAS. The switching frequency kept constant by keeping the reference voltages of the SVPWM are smoother. This is because dividing the error in the stator flux at the sampling of the switching time, which reflecting on the performance characteristics of the PMSM. This means that any variation in the smoother voltage of the input of the SVPWM will reflect on the ripples in the motor torque, the noise in the stator flux, the total harmonic distortion of the stator current and noise in the motor speed. This means that more improvement in the performance of the PMSM if it is compared to the motor performance with both classical model and the modified model. This voltage can be estimated through eq. (12). This voltage is used as the input voltage of the SVPWM which generated pulses to drive the inverter voltage which applied on the PMSM to drive it.

$$V^{*}_{abc} = \frac{\Delta\lambda}{\Delta T} + R_s I_{abc} \qquad (12)$$

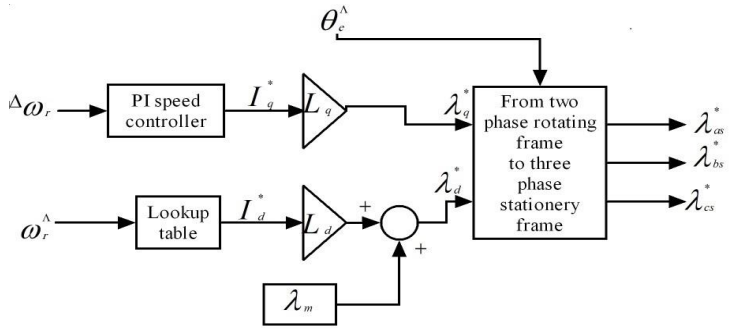

Figure 10 Details of the stator flux estimator through vector block

Simulation results

The motor parameters used in this simulation can be seen in appendix I. To study the effect of

the proposed model on the motor performance, the motor in this simulation will run at constant load different speeds e.g., low speed, rated speed and above rated speed. The torque ripples, total harmonic distortion (THD), rise time, settling time and maximum overshooting of the motor speed were recorded in tables IV and V respectively to show the effectiveness of the proposed model. The figures and tables which explained this can be seen in the following;

The figures 11-13 show the variation of the motor currents under the effect of the study models where it is found that at low speed, the stator current is highly distorted with modified model. When nearest to the rated speed and above the classical model is highly distorted. Also, the best performance in the stator current occurred with the proposed model at any speed.

Figures 14-16 show the improvement of the motor torque with the proposed model compared to the other models where it is found that the highest ripples in the motor torque occurred with the modified model at low speed. At nearest rated speed and above, the classical model recorded highest ripples and these ripples improved with modified model. Also, at any motor speed with the proposed model it was found that the torque ripples are more improvement.

Figures 17-19 show the shape of the motor speed with sensorless control where it is found that highest noise occurred with modified model at low speed. At nearest rated speed and above, the classical model recorded highest noise and this noise improved with modified model. Also, at any motor speed with the proposed model it was found that the noise in the motor speed are more improvement.

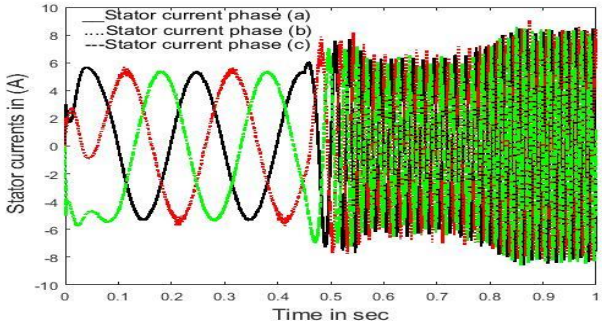

Figure 11 Stator currents with classical model

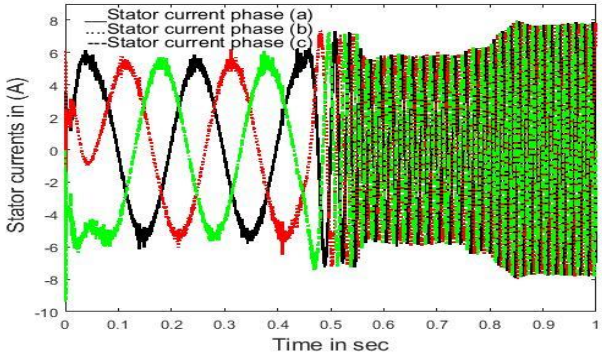

Figure 12 Stator currents with modified model

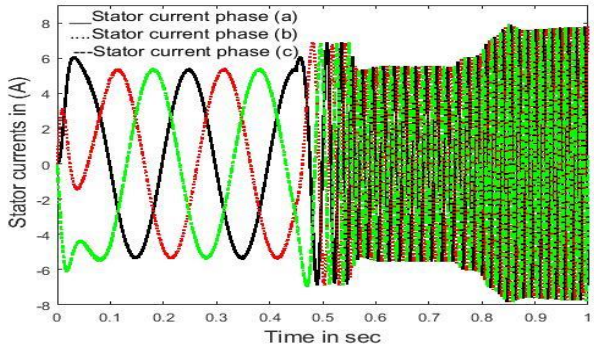

Figure 13 Stator currents with proposed model

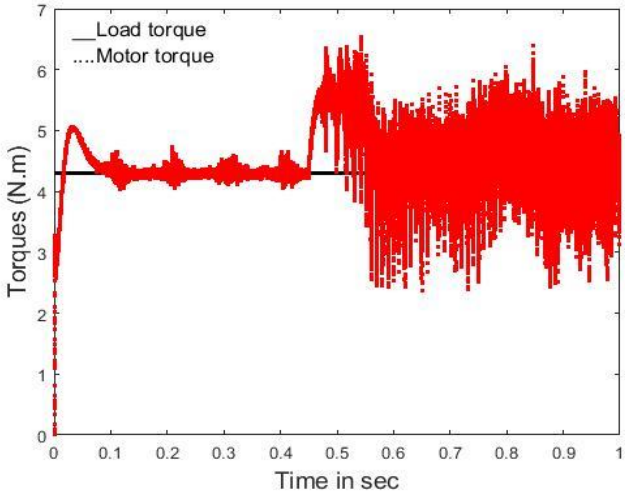

Figure 14 Motor torque with classical model

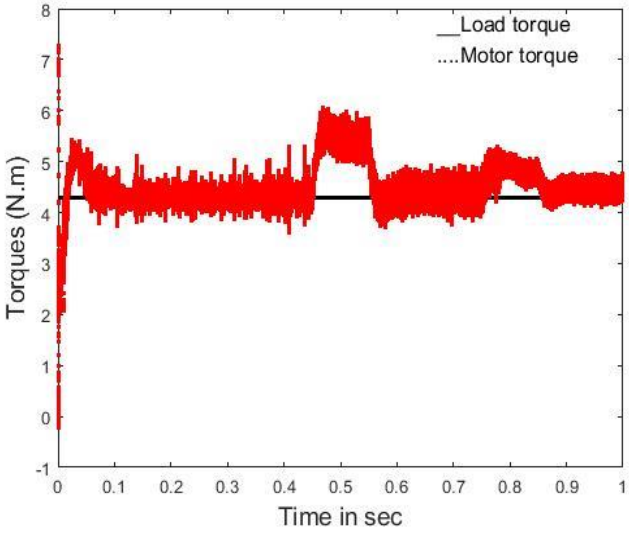

Figure 15 Motor torque with modified model

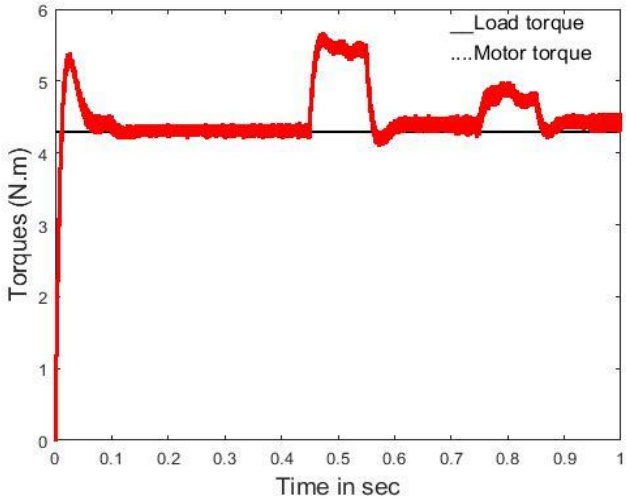

Figure 16 Motor torque with proposed model

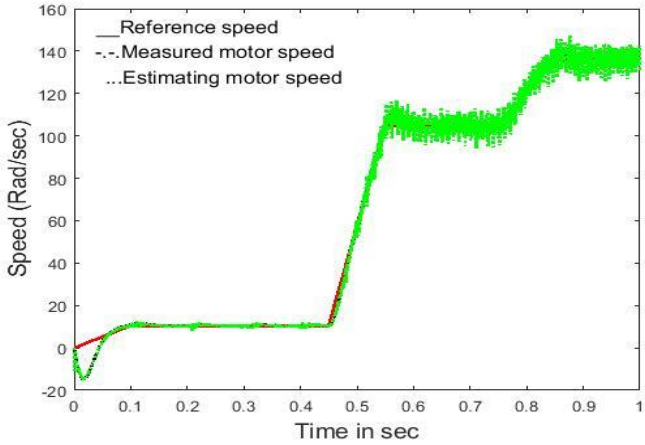

Figure 17 Motor speed with classical model

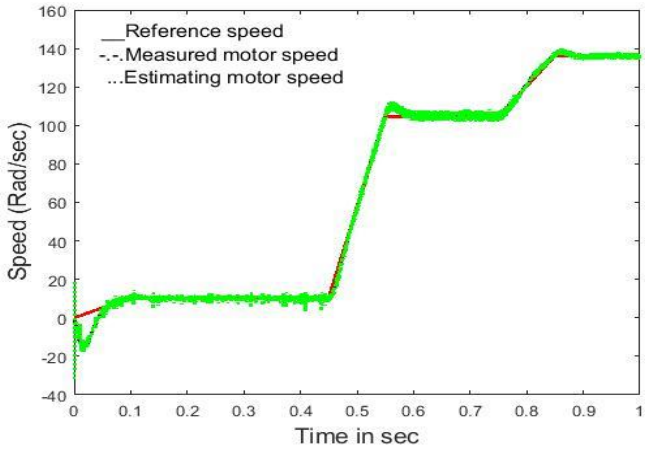

Figure 18 Motor speed with modified model

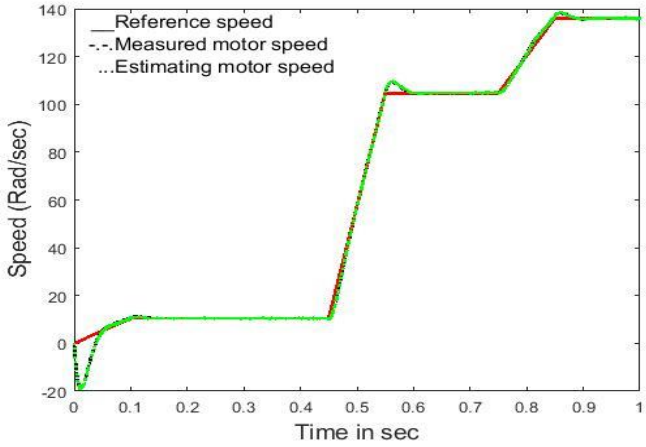

Figure 19 Motor speed with proposed model

Table IV The THD and torque ripples of the model under study

Type of the system	THD %			Torque ripples %		
	Low speed	Rated speed	Above rated speed	Low speed	Rated speed	Above rated speed
Classical system	1.4	7.24	4.74	2	16.42	13.54
Modified model	3.55	3.81	1.87	4.7	4.91	3
Proposed model	0.81	0.74	0.83	0.86	0.75	0.96

Table V The raise time, maximum overshooting settling time for the model under study

Type of the system	Low speed			Rated speed			Above rated speed		
	Raise time in sec	Maximum over shooting %	Settling time in sec	Raise time in sec	Maximum over shooting %	Settling time in sec	Raise time in sec	Maximum over shooting %	Settling time in sec
Classical system	0.078	131.15	0.25	0.54	112.7	0.62	0.8	106.52	0.88
Modified model	0.06	129.1	0.18	0.48	107.9	0.6	0.78	102.8	0.87
Proposed model	0.077	109.8	0.128	0.54	105.04	0.59	0.8	102.1	0.88

CONCLUSION

This paper studied the sensorless problems through vector control. It was suggested proposed model to improve these problems. The proposed model improves the performance characteristics of the PMSM overall where the THD, torque ripples and maximum overshooting decreased when the motor operated under low frequency, rated frequency and above the rated frequency. The proposed model depends upon replacing the two-level inverter by three level inverter and keeping the switching frequency of the inverter is constant.

Appendix I

Line to line voltages	110V
Inertia	0.001118Kg.m2
Magnetic flux linkage	0.108Wb
Poles	6
Rated power	900W

Rated speed	1000 R.P.M
Stator resistance	0.43ohm
q-axis inductance	6.97mH
d-axis inductance	6.97mH

REFERENCES

Tingting Liu, Guojin Chen and Shigang Li, 2014. Application of Vector Control Technology for PMSM Used in Electric Vehicles. The Open Automation and Control Systems Journal. **6**:1334-1341.

Kangping Xu, Wenjia Chen, Yushan Xu, Mingyu Gao, Zhiwei He, 2014. Vector Control for PMSM. Sensors & Transducers. **170**: 227-233.

Shweta Singh, Amjad Anvari-Moghaddam, 2018. Sensor-based and Sensorless Vector Control of PM Synchronous Motor Drives: A Comparative Study.4th IEEE Southern Power Electronics Conference. Singapore.

Omer Cihan Kivanc, and Salih Baris Ozturk, 2018. Low-Cost Position Sensorless Speed Control of PMSM Drive Using Four-Switch Inverter. energies. **10**: 1-24.

Sandeep V Nair, IIT Madras, Kamalesh Hatua; NVPR Durga Prasad; D Kishore Reddy, 2018. A Smooth and Stable Open-Loop I-F Control for a Surface Mount PMSM Drive by Ensuring Controlled Starting Torque. 44th Annual Conference of the IEEE Industrial Electronics Society. Washington, DC, USA.

Shoeb Hussain and Mohammad Abid Bazaz; 2016. Sensorless Control of PMSM Drive using Neural Network Observer, International Conference on Power Electronics. Intelligent Control and Energy Systems. Delhi, India.

Abolfaz Halvaei Niasar, Hossein Rahimi Khoei, Mahdi Zolfaghari, Hassan Moghbeli, 2015. Artificial Neural Network based Sensorless Vector Control of Induction Motor Drive. Applied Mechanics and Materials **704**: 325-328

Yuxin Li, Gaolin Wang, Wen Shen, Guoqiang Zhang, Nannan Zhao, Xintian He, Dianguo Xu, 2020. High-Frequency Signal Injection using Extend State Observer for Position Sensorless PMSM Drives. IEEE Conference on Industrial Electronics and Applications. Kristiansand, Norway.

Shoeb Hussain and Mohammad Abid Bazaz, 2014. Sensorless Control of PMSM using Extended Kalman Filter with Sliding Mode Controller. IEEE International Conference on Power Electronics, Drives and Energy Systems. Mumbai, India.

Sandeep V. Nair, Kamalesh Hatua, N.V.P.R. Durga Prasad, D. Kishore Reddy; 2020. Quick and seamless transition method for I-f to sensorless vector control changeover and on-the-fly start of PMSM drives.IET Electric Power Applications. **14**: 2231-2242.

Qing-wei Luo; Su-dan Huang; Guang-zhong Cao, 2013. Sensorless vector control of permanent magnet synchronous motors based on the improved sliding mode observer. 5th International Conference on Power Electronics Systems and Applications. Hong Kong, China.

Hongguo Li, Dongliang Ke, Ran Zu, Peng Tao, Fengxiang Wang; 2018. Sensorless Control of Permanent Magnet Synchronous Motor Based on An Improved Sliding Mode Observer.2018 IEEE Student Conference on Electric Machines and Systems. Huzhou, China.

Abbas Mahmood Oghor Anwer, Fuad Alhaj Omar, and Ahmet Afsin Kulaksiz; 2020. Design of a Fuzzy Logic-based MPPT Controller for a PV System Employing Sensorless Control of MRAS-based PMSM. International Journal of Control, Automation and Systems. **18**: 1-10.

Zhewen Tian and Kaiyuan Shen, 2020. Research on Sensorless Control System of PMSM Based on Adaptive Fuzzy Sliding Mode Observer. Journal of Physics. **12**: 1-9.

AMOR KHLAIEF, MOHAMED BOUSSAK and MONCEF GOSSA; 2013. Model Reference Adaptive System Based Adaptive Speed Estimation for Sensorless Vector Control with Initial Rotor Position Estimation for Interior Permanent Magnet Synchronous Motor Drive

AMOR KHLAIEF. Electric Power Components and Systems, **41**: 47-74.
Hamdy Mohamed Soliman, 2019.Improve the performance characteristics of the IPMSM under the effect of the varying loads. IET Electric Power Applications. **13**: 1935-1945.
Zulkifilie Bin Ibrahim, Md. Liton Hossain, Syamim Binti Sanusi, Nik Munaji Bin Nik Mahadi, Ahmad Shukri Abu Hasim, 2014. Performance of Different Topologies for Three Level Inverter Based on Space Vector Pulse Width Modulation Technique. IET International Conference on Clean Energy and Technology Kuching.